Alexandria Engineering Journal (2020) 59, 4577–4592

HOSTED BY

ELSEVIER

Alexandria University

Alexandria Engineering Journal

www.elsevier.com/locate/aej
www.sciencedirect.com

Reliability-based topology optimization using inverse optimum safety factor approaches

G. Kharmanda [a], S. Gowid [b,*], A. Shokry [c]

[a] Mechanics Laboratory of Normandy, INSA Rouen, St Etienne du Rouvray, France
[b] Department of Mechanical and Industrial Engineering, Qatar University, Doha, Qatar
[c] Department of Mechanical Engineering, Fayoum University, Fayoum 63514, Egypt

Received 24 February 2020; revised 17 July 2020; accepted 12 August 2020
Available online 9 September 2020

KEYWORDS

Deterministic topology optimization;
Reliability-based topology optimization;
Inverse optimum safety factor

Abstract The Deterministic Topology Optimization (DTO) model generates a single solution for a given design space, while the Reliability-Based Topology Optimization (RBTO) model provides several reliability-based topology layouts with high performance levels. The objective of this work is to develop two approaches, which can lead to two new topology categories. The two alternative approaches; namely Objective-Based Inverse Optimum Safety Factor (IOSF) and Performance-Based IOSF, are developed based on the IOSF. When designing a structure, the uncertainty in the input parameters influences the output parameters and thus a sensitivity analysis was carried out for the developed approaches. The analysis shows the influence of each parameter on the structure performance. Two numerical applications are presented to show the effectiveness of the developed approaches. When considering a certain reliability level, unlike the DTO, the RBTO results in different configurations. Unlike the results of the previous studies, the consideration of the geometry uncertainty reveals that the structural volume increases as the reliability level increases. Additionally, the developed approaches can be considered as two generative tools that can produce two different categories/families of solutions.

1. Introduction

The objective of the topology optimization is to answer one of the first questions of the structure nature to fulfill the necessary technical specifications. This way the problem is to determine the structure's general characteristics, and to make that initial choice as automatically as possible [1]. Furthermore, in topology optimization, both macroscopic structures and microscopic materials can be treated [2].

In the literature, two topology optimization models can be generally distinguished: Deterministic Topology Optimization (DTO) and Reliability-Based Topology Optimization (RBTO). In the DTO model, a single configuration for a given space can be determined [3], while using the RBTO model, several configurations can be found with different advantages. This enables the selection of the best resulting topology that fulfills the required technical specifications. The structural weight of the resulting configurations obtained by the RBTO model is minimized compared to the DTO model [4-8]. In addition to that,

* Corresponding author.
E-mail address: samer@qu.edu.qa (S. Gowid).
Peer review under responsibility of Faculty of Engineering, Alexandria University.

https://doi.org/10.1016/j.aej.2020.08.013

when using the RBTO model and even for the same structural weight, the obtained configuration is found more reliable than the deterministic one [9]. The different RBTO works can be classified according to two points of view: topology optimization and reliability analysis. The interested reader can find a detailed review in Kharmanda et al. [10]. It has been found that the different developments from a point of view 'topology optimization' seem to be interesting for topology designers, because it provides several reliability-based structures with respect to the reliability index changes. It leads to different layouts, while the developments from a point of view 'reliability analysis' leads to the same layout structures with different densities that have no sense for the following optimization stages [11-13,15-17,28].

To model the uncertainty in the topology optimization from a point of view 'topology optimization', Kharmanda and Olhoff [4] were the first researches who introduced reliability constraints into deterministic topology optimization problems. The algorithm of their proposed Gradient-Based Method (GBM) starts with the sensitivity evaluation with respect to the different variables to identify the random variables that have large influence on the objective function. The importance of the RBTO model is to provide structures that are more reliable than those generated by DTO (see also [5-7]). After that, Patel and Choi [18] applied probabilistic neural networks in the case of highly nonlinear problems. Next, Wang et al. [19] developed a non-probabilistic approach for detailed design of continuum structures, in which the unknown But Bounded Uncertainties (BBU) that exist in material as well as external loads are simultaneously considered. Recently, in Kharmanda et al. [10], the Inverse Optimum Safety Factor (IOSF) was proposed to deal with the modal analysis where there is no applied load and the integration of topology optimization into free vibrated structures may lead to unrealistic topologies. The application of the IOSF method was limited to consider the parameterization only on the geometry of the optimization domain.

To perform the RBTO problems, many Reliability-Based Design Optimization (RBDO) techniques can be considered. Several RBDO methods have been developed regarding to their application fields [20]. For example, the Optimum Safety Factor (OSF) method has been simply implemented considering two main stages [21]. The first stage is to identify the failure point using a simple optimization procedure, while in the second stage, the OSF formulations are used to evaluate the optimum solution. This method has shown its efficiency on the nonlinear distribution cases [22]. Due to its simple implementation, the OSF method has shown its efficiency on several industrial applications by other researchers [23,24]. The OSF is developed for detailed design stage (for example sizing and shape optimization). The integration of reliability concept into sizing and shape optimization is easy since all of them are quantitative of nature. However, the topology optimization which belongs to the conceptual design stage, is not quantitative of nature. So, the integration of reliability concept into topology optimization was a big challenge [4] and needs special procedures processes. This way the RBTO was previously performed using the GBM which is a special optimization technique [4-7] where the limit state function was modeled as a simple linear combination of random variables and the structural compliance was considered as an objective function. This simplification was considered by several researchers as a serious drawback when dealing with realistic failure probability problem [25]. In the work of Mozumder et al. [25], when considering the structural volume as an objective function, the resulting reliability-based topologies had the same geometry descriptions with different dimensions, while the method proposed in this paper leads to different geometry descriptions, which represents a significant design tool to the topology designers. Accordingly, there is a strong need to overcome these drawbacks with the consideration of the nonlinearity of the failure probability problems.

In this work, the basic idea of the OSF method is considered to develop two alternative IOSF approaches in order to overcome the mentioned drawbacks and to provide the best coupling between reliability analysis and topology optimization which are different of nature (quantitative and non-quantitative). Therefore, two alternative IOSF approaches are developed to mitigate the drawbacks of the previous research. These new approaches help produce two categories/families of solutionsthat can give many possibilities for the designers and helps them to select the best configuration that can give the most advantageous solution for their problem. The resulting topology layouts are controlled by a given design space (loading, material, geometry ...). Two numerical applications (2D & 3D) are detailed where the topology optimization problem is modeled in two different ways. In the first application, the study is carried out on a simple MBB (Messerschmitt-Bölkow-Blohm) beam with two holes considering the uncertainty on the input parameters (loading and material properties) and the output parameters (volume decrease ratio or compliance increase ratio). In the second application, the geometry uncertainty is added to show its effect on the different functions (compliance and volume). The studied 3D case gives the opportunity to apply the uncertainty on several geometrical parameters without affecting the structure performance, while applying the uncertainty of the dimensions of the MBB beam or its two holes can affect the boundary conditions and then the structure performance.

2. Materials and methods

2.1. Deterministic topology optimization (DTO) methods

In this work, the topology optimization problem is solved using two different methods: The first method is to minimize the compliance, subject to a target decrease ratio of the structural volume V_f. The DTO problem can be mathematically formulated as follows:

$$\begin{aligned} &\min : C(\mathbf{x}) \\ &s.t. : \tfrac{V(\mathbf{x})}{V^0} \leqslant V_f \end{aligned} \tag{1}$$

where $C(\mathbf{x})$ is the compliance considering the material densities in each element as optimization variables which belong to the interval [0,1]. $V^0$and $V(\mathbf{x})$ are the initial- and current structural volume values. The second method is to minimize the structural volume, subject to a target increase ratio of the compliance C_f. The DTO problem can be mathematically formulated as follows:

$$\begin{aligned} &\min : V(\mathbf{x}) \\ &s.t. : \tfrac{C(\mathbf{x})}{C^0} \leqslant 1 + C_f \end{aligned} \tag{2}$$

where $V(\mathbf{x})$ is the structural volume considering the material densities in each element as optimization variables which belong to the interval [0,1]. $C^0$and $C(\mathbf{x})$ are the initial- and current compliance values. Formulations 1 and 2 are basic forms and can be used with several topology optimization methods such as SIMP (Solid Isotropic Microstructure with Penalty) [26].

2.2. Reliability methods

To evaluate the reliability level, the First and the Second Order Reliability Methods FORM/SORM have been proposed. Both of these methods are important in structural reliability application, especially for risk assessment [14,27]. However, in this work, the reliability concept is only used at the conceptual design stage which is represented by the topology optimization procedure. So, FORM is used in a simple way to be integrated with topology optimization.

In order to control the resulting topologies, a reliability indexβ is introduced with a normalized vector $\mathbf{u}$ [4]. Fig. 1 shows the transformation between the random variables $\mathbf{y}$ in the physical space (Fig. 1a) and the normalized vector $\mathbf{u}$ in the normalized space (Fig. 1b). The general evaluation of the reliability index can be realized by the following optimization problem:

$$\begin{aligned} &\beta = \min d(\mathbf{u}) \\ &s.t : H(u) \;=\; 0 \end{aligned} \tag{3}$$

where the distance $d(\mathbf{u})$is given by:

$$d(\mathbf{u}) = \sqrt{u_1^2 + \ldots + u_n^2} \tag{4}$$

The optimum value of β (minimum distance) corresponds to the Most Probable failure Point (MPP). The evaluation of the reliability index is carried out by FORM (First Order Reliability Method).

The effect of the reliability index values plays an important role in the conceptual design stage. The validation of this effect is recently studied by Kharmanda et al. [10]. In general, the nuclear and spatial applications necessitate a very small value of failure probability, the failure probability has to be: $P_f \in [10^{-6} - 10^{-8}]$ which corresponds to a reliability index $\beta \in [4.75 - 5.6]$, while in structural engineering, the failure probability has to be: $P_f \in [10^{-3} - 10^{-5}]$ which corresponds to a reliability index $\beta \in [3 - 4.25]$. The interested reader can refer to a detailed study of target safety indices in [29,30].

2.3. Reliability-Based topology optimization (RBTO) methods

In general, there is a big difference between the reliability and the reliability-based optimization approaches. When dealing with a simple reliability evaluation, direct algorithms can be used, while the reliability-based optimization (RBDO & RBTO) procedures are generally composed of two nested problems. The use of classical reliability algorithms may lead to several difficulties such as high computing time and convergence stability [20,21] Therefore, it is the objective to developed new efficient methods to be suitable for this kind of reliability-based optimization problems.

In our previous works [4-8], a decoupled RBTO technique so-called Gradient-Based Method (GBM) had been developed where the reliable design was achieved by implementing the reliability analysis at the beginning of the optimization process. The advantage of the GBM is to provide several solutions with respect to the reliability index values compared to the developments from a point of view 'reliability analysis' [25,31]. In this paper, two different strategies based on a sensitivity study are developed.

2.3.1. RBTO by Objective-Based IOSF Approach

The previous OSF method can efficiently reduce the size of the RBDO problem using the sensitivities of the limit state with respect to all the structure's variables, especially when the sensitivity can be evaluated analytically [32]. The basic idea of the classical OSF method used in RBDO applications is to find the

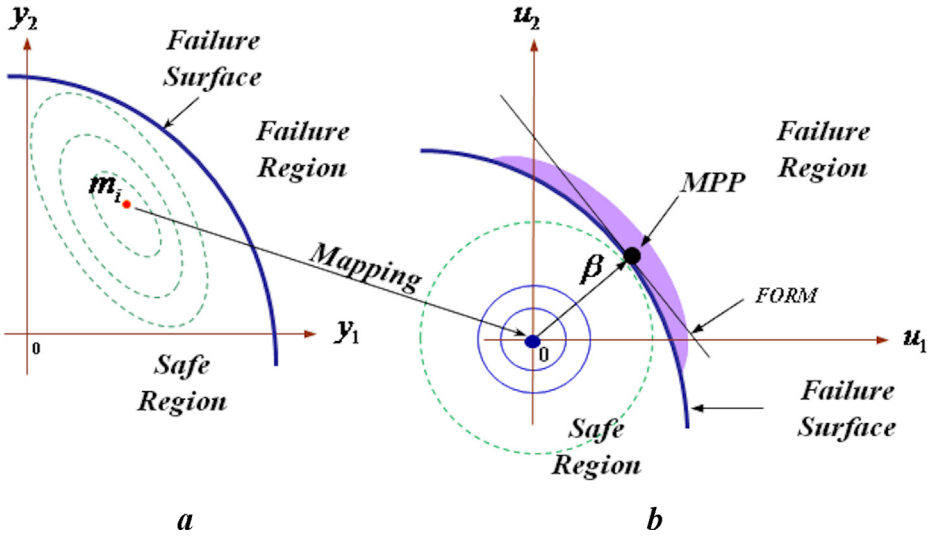

Fig. 1 Transformation between a) the physical space and b) the normalized space.

failure point and next the optimum solution using the OSF formulations [23]. The RBTO problem aims to minimize the compliance, subject to a target decrease ratio of the structural volume V_f and the reliability constraint. The RBTO problem can be mathematically formulated as follows:

$$\begin{aligned} &\min : C(\mathbf{x}) \\ &s.t. : \tfrac{V(\mathbf{x})}{V^0} \leqslant V_f \\ &and : \beta \geqslant \beta_t \end{aligned} \tag{5}$$

where β_t is the target (required) reliability index to be respected. The failure is related to the compliance which is considered as an objective function. Thus, the sensitivity can be estimated considering the objective function as a failure criterion. This way the optimum value of the normalized vector can be written in the following form:

$$u_i^* = \beta_t \sqrt{\frac{\left|\frac{\partial F}{\partial y_i}\right|}{\sum_{j=1}^{n}\left|\frac{\partial F}{\partial y_j}\right|}} \tag{6}$$

where the sign of $\pm$ depends on the sign of the sensitivity of the objective function with respect to random vector y_i, i.e.,

$$\frac{\partial F}{\partial y_i} > 0 \Longleftrightarrow u_i^* > 0 \text{ and } \frac{\partial F}{\partial y_i} < 0 \Longleftrightarrow u_i^* < 0 \ , i = 1, ..., n \tag{7}$$

where F is the objective function represented by the compliance. This method takes into account both concepts of the OSF and failure criterion. When the failure criterion is treated as an objective function, the Objective-Based IOSF Approach can be implemented. However, when the failure criterion is treated as a performance function, the method can be called Performance-Based IOSF Approach, which is presented in the next section.

2.3.2. RBTO by Performance-Based IOSF Approach

The different RBDO developments of the OSF method for linear and nonlinear distribution laws are carried out considering the structural reliability philosophy [23]. These developments fit with the basic idea of this proposed method where the compliance is considered as a performance function (constraint function). Thus, the RBTO problem aims to minimize the structural volume subject to the compliance constraint and the reliability constraint. The RBTO problem can be mathematically formulated as follows:

$$\begin{aligned} &\min : V(\mathbf{x}) \\ &s.t. : \tfrac{C(\mathbf{x})}{C^0} \leqslant 1 + C_f \\ &and : \beta \geqslant \beta_t \end{aligned} \tag{8}$$

The optimum value of the normalized vector can be written in the following form:

$$u_i^* = \beta_t \sqrt{\frac{\left|\frac{\partial G}{\partial y_i}\right|}{\sum_{j=1}^{n}\left|\frac{\partial G}{\partial y_j}\right|}} \tag{9}$$

where the sign of $\pm$ depends on the sign of the sensitivity of the limit state function with respect to random vector y_i, i.e.,

$$\frac{\partial G}{\partial y_i} > 0 \Longleftrightarrow u_i^* > 0 \text{ and } \frac{\partial G}{\partial y_i} < 0 \Longleftrightarrow u_i^* < 0 \ , i = 1, ..., n \tag{10}$$

where G is the objective function represented by the compliance. This method treated the compliance as a performance function. The main difference between this method and the classical OSF in RBDO model is the sign of the derivative. Both proposed methods provide different solutions.

2.4. Distribution laws

The OSF formulation has been developed considering the most common distribution laws in the RBDO studies (normal, log-normal, uniform, Weibull and Gumbel). In this work, the normal distribution law is considered and hence the random variable vector follows the normal distribution law. Thus, the safety factor can be written as follows [22,33,34]:

$$S_{f_i} = 1 + \gamma_i \cdot u_i^* \tag{11}$$

where the variance coefficient γ_i relates the mean m_i and standard-deviation σ_i by the following expression:

$$\gamma_i = \sigma_i / m_i \tag{12}$$

In both developed approaches, the starting point is considered as a failure point P_y^*, and next a reliability-based topology P_x^* is found to be more reliable than the first solution P_y^* considering a required reliability level β_t. So the failure point P_y^* is found by a DTO procedure and the reliability-based topologies P_x^* are found using the both developed approaches. In this work, the target reliability indices are: $\beta_t = 3$ which corresponds to the first point of the safety interval ($\beta \in [3 - 4.25]$) and $\beta_t = 3.8$ which is the used target reliability index for many structural engineering applications [30].

3. Results and discussion

3.1. MBB beam with two holes (2D model)

In this case, the topology optimization is applied to a 2D MBB beam with two holes. Here, two studied optimization problems are considered: The first optimization problem is to minimize the structural compliance $C(\mathbf{x})$ subject to the constraint of the volume decrease ratio V_f (Eqs (1) and (5)). While, the second optimization problem is to minimize the structural volume $V(\mathbf{x})$ subject the constraint of the compliance increase ratio C_f (Eqs (2) and (8)). It is the objective to alert between the compliance and the volume functions as objective and performance functions.

The objective is to find the best distribution of material considering three studies: DTO and RBTO using Objective-Based IOSF approach, and RBTO using Performance-Based IOSF approach.

The initial domain is represented by a rectangle (1×0.4m) with two holes where the diameter is: 0.16 m. All other dimensions are shown in Fig. 2 in meters. The material of this beam is steel, which has a Young's modulus $E = 200000$(MPa) and a Poisson's ratio $v = 0.3$. The material behavior is linear elastic isotropic. The applied force is: $F = 1000$ N. The boundary conditions are shown in Fig. 2. The number of elements can affect the resulting topology. In Kharmanda and Olhoff [4], the randomness was considered on the number of elements in the horizontal and vertical directions. However, in this work, a free mesh technique called Smart-Mesh is used. This

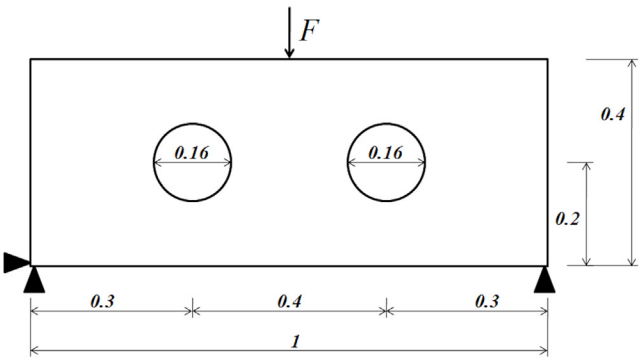

Fig. 2 Initial configuration of the studied 2D MBB beam with two holes.

technique is implemented in ANSYS and help to improve the result quality.

To perform the RBTO using both Objective-Based and Performance-Based IOSF Approaches, a sensitivity evaluation is required on the starting point configuration using the central finite difference approach as an accurate tool for sensitivity analysis [35]. Two categories of solutions are distinguished:

3.1.1. First category of solutions for the studied MBB beam with two holes

The starting configuration is considered to be the failure point where the problem is to minimize the compliance subject to the volume constraint for the DTO (Eq. (1)) and also the reliability constraint for the RBTO (Eq. (5)). The used method for this kind of topology optimization problems, is the Optimality Criteria (OC) implemented in ANSYS Software.

Fig. 3a, b and c show the resulting topologies when considering the compliance as an objective function for DTO model (failure point P_y^*) and for RBTO models using Objective-Based IOSF approach when the target reliability indices are: $\beta_t = 3$, and $\beta_t = 3.8$. These target values are selected according to different structural engineering application [30]. In fact the layouts change when the reliability index value increases, in which some parts that colored in red and represent the full material distribution start to disappear. For example, the configuration around the two holes is found different (see Fig. 3a, b, and c). When considering the compliance as an objective function, the increase of the reliability index values leads to change of resulting reliability-based topologies which confirm our previous findings [4-7].

The corresponding resulting compliances are shown in Table 1 for the initial configuration C^0 and the optimal one C^*. The used number of element for optimization is 3855 nonlinear elements (PLANE82, 8-node). The uncertainty is considered on the material properties (E and ν), the loading (F) and the volume decrease ratio (V_f). The four random variables are then: F, E, ν and V_f. The standard deviations are assumed to be proportional to the starting values (P_y^*) presented in Table 1, i.e. $\sigma_i = \gamma_i m_i$ (Eq. (12)) where $\gamma_i = 0.1$.

Table 1 presents the input and output parameters of the DTO and RBTO studies for the first category of solutions for the studied MBB beam with two holes. It is shown for the RBTO results that the reduction of the structural volume

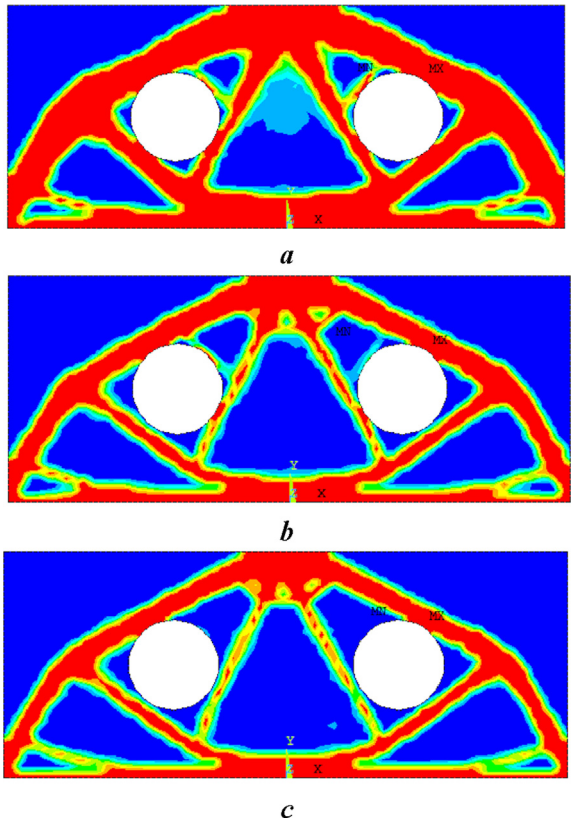

Fig. 3 Resulting 2D topologies when considering the compliance as an objective function: a) DTO configuration, b) RBTO configuration for $\beta_t = 3$, and c) RBTO configuration for $\beta_t = 3.8$.

is almost 10%, while the increase of the structural compliance is almost 16%.

As shown in Fig. 3, the resulting reliability-based topologies can be modeled with different layouts for the next stage (detailed design). When increasing the reliability index value, different topologies are obtained (Fig. 3b and c). This observation is numerically supported by the decrease of the structural volume $V(\mathbf{x})$, when increasing the reliability index values (see Table 1).

Fig. 4 shows the sensitivity magnitude value of the compliance that is considered as an objective function. The figure shows that the effect of the volume decrease ratio is more than three times compared to the effect of force. It is found that the volume decrease ratio V_f has the biggest effect on the resulting compliance, while the Poisson's ratio has no influence on the resulting compliance as shown in Fig. 4.

3.1.2. Second category of solutions for the studied MBB beam with two holes

The starting configuration is considered to be the failure point where the problem is to minimize the volume subject to the compliance constraint for the DTO (Eq. (2)) and also the reliability constraint for the RBTO (Eq. (8)). The used method for this kind of topology optimization problems, is the Sequential Convex Programming (SCP) implemented in ANSYS Software.

Fig. 5a, b and c show the resulting topologies when considering the compliance as a performance function for DTO

Table 1 DTO and RBTO results for the first category of solutions for the studied MBB beam with two holes.

Parameters	P_y^*	$\beta_t = 3$			$\beta_t = 3.8$		
		u_i	S_{f_i}	P_x^*	u_i	S_{f_i}	P_x^*
F(N)	1000	1.02593	1.102593	1102.593	1.29951	1.129951	1129.951
E(MPa)	200,000	0.0513	0.99487	198,974	0.06498	0.993502	198700.4
v	0.3	0	1	0.3	0	1	0.3
V_f	50	2.81866	1.281866	64.09329	3.5703	1.35703	67.8515
C^0(N.m)	255.179	541.973			685.468		
C^*(N.m)	87.2253	141.274			163.798		
$V(\mathbf{x})(m^3)$	0.179894	0.129188			0.115666		

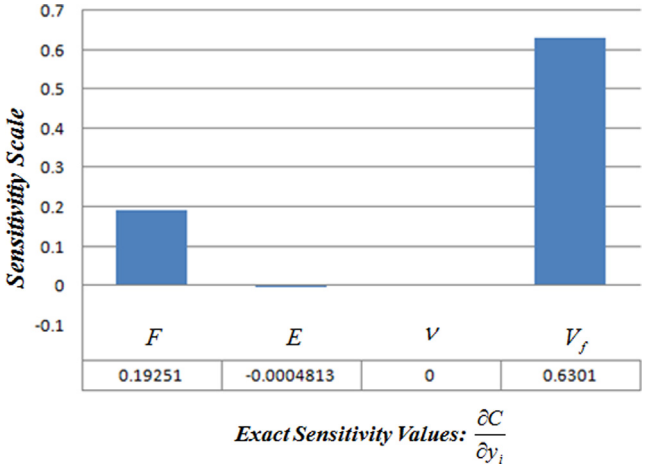

Fig. 4 Sensitivity magnitude values of the compliance as an objective function.

model (failure point P_y^*) and for RBTO models when the target reliability indices are: $\beta_t = 3$, and $\beta_t = 3.8$. The figure shows that there is almost no difference between the three subfigures. These results are similar to the developments of Mozumder et al. [25] where the structural volume is considered as an objective function and the structural compliance as a performance function.

The corresponding resulting volumes are shown in Table 2 for the initial configuration V^0 and the optimal one V^*. The used number of element for optimization is 3855 nonlinear elements (PLANE82, 8-node). The uncertainty is considered on the material properties (E and v), the loading (F) and the compliance increase ratio (C_f). The random variables are then: E, v, F and C_f. The standard deviations are assumed to be proportional to the starting values (P_y^*) presented in Table 2, i.e. $\sigma_i = \gamma_i m_i$ (Eq. (12)) where $\gamma_i = 0.1$.

Table 2 presents the input and output parameters of the DTO and RBTO studies for the second category of solutions for the studied MBB beam with two holes. It is shown for the RBTO results that the reduction of the structural volume is almost 2.4%, while the increase of the structural compliance is almost 9.4%.

Fig. 6 shows the sensitivity magnitude values of the compliance that is considered as a performance function. Here, the effect of the material properties can be ignored and the compliance increase ratio C_f plays an important role in the compliance. The compliance increase ratio $C_f$has also the biggest influence on the resulting compliance and the Poisson's ratio has no effect on the resulting compliance. The figure shows that the effect of the compliance increase ratio is more than seven times compared to the effect of the force.

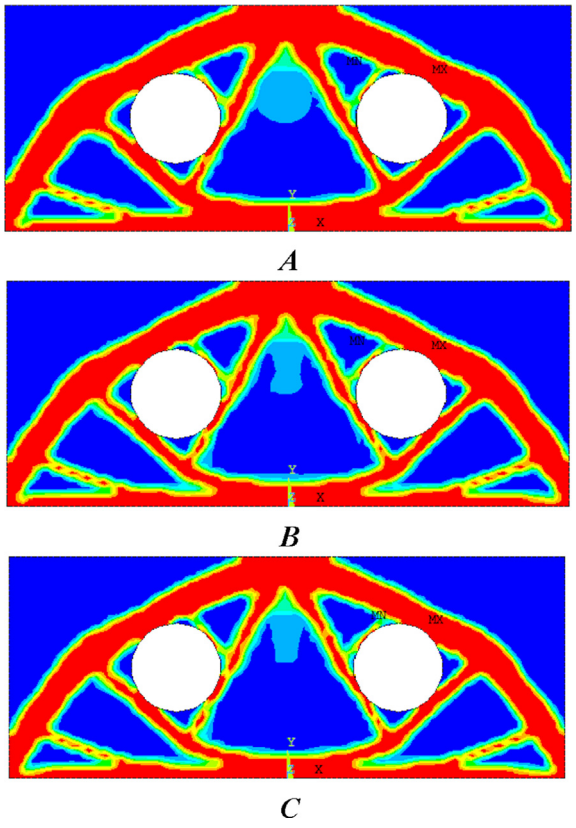

Fig. 5 Resulting 2D topologies when considering the compliance as a performance function: a) DTO configuration, b) RBTO configuration for $\beta_t = 3$, and c) RBTO configuration for $\beta_t = 3.8$.

When using the Performance-Based IOSF Approach, the difference between the biggest and smallest values of the sensitivity is smaller than that produced by the Objective-Based IOSF Approach (see Figs. 4 and 6).

Fig. 7a and b show a comparison between the compliance and the volume values for the first and the second categories

Table 2 DTO and RBTO results for the second category of solutions for the studied MBB beam with two holes.

Parameters	P_y^*	$\beta_t = 3$			$\beta_t = 3.8$		
		u_i	S_{f_i}	P_x^*	u_i	S_{f_i}	P_x^*
F(N)	1000	1.45085	1.145085	1145.085	1.83775	1.183775	1183.775
E(MPa)	200,000	0.07254	0.992746	198549.1	0.09189	0.990811	198162.2
v	0.3	0	1	0.3	0	1	0.3
C_f	50	2.62483	1.262483	63.12417	3.32479	1.332479	66.62395
V^0(m^3)	0.359788	0.359788			0.359788		
V^*(m^3)	0.157306	0.142554			0.139161		
C(**x**)(N.m)	96.2535	138.243			151.227		

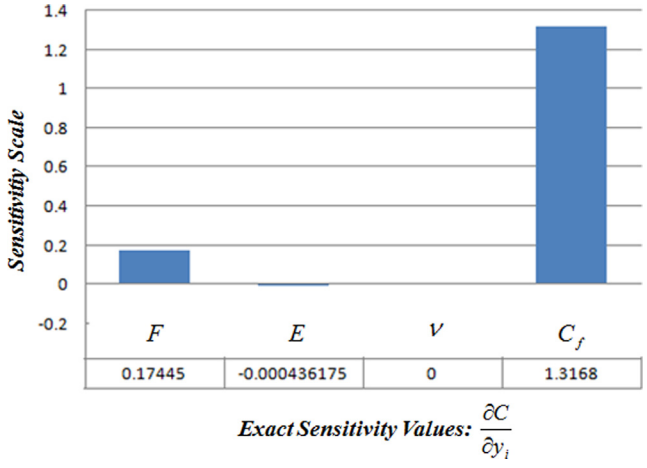

Fig. 6 Sensitivity magnitude values of the compliance as a performance function.

of solutions for the studied MBB beam with two holes. According to Fig. 7a and b, when increasing the reliability index values, the resulting compliance values increases while the resulting structural volume values decreases.

As result, when using the Objective-Based IOSF Approach, the compliance is treated as an objective function and its sensitivity is evaluated with respect to four parameters. This way a first RBTO solution category is obtained when changing the reliability index values. However, when using the Performance-Based IOSF Approach, the compliance is treated as a performance function and its sensitivity is evaluated with respect to four parameters. A second RBTO solution category is obtained when changing the reliability index values. When changing the reliability index values, a small difference is observed between the resulting RBTO layouts (Fig. 5b and c) compared to those produced by the Objective-Based IOSF Approach (Fig. 3b and c). The numerical results in Table 2 show that the optimal values of the structural volume V^* decrease when increasing the reliability index values.

3.2. Bridge structure (3D model)

In this case, the topology optimization is applied to a 3D bridge structure considering two studied optimization cases: The first optimization case is to minimize the structural compliance $C(\mathbf{x})$ subject the constraint of the volume decrease ratio V_f (Eqs (1) and (5)). While, the second optimization case is to minimize the structural volume $V(\mathbf{x})$ subject the constraint of the compliance increase ratio C_f (Eqs (2) and (8)). The objective is to find the best material distribution considering three studies: DTO, RBTO using Objective-Based IOSF approach, and RBTO using Performance-Based IOSF approach.

The initial domain is divided to optimized and non-optimized domains as shown in Fig. 8. The dimensions of

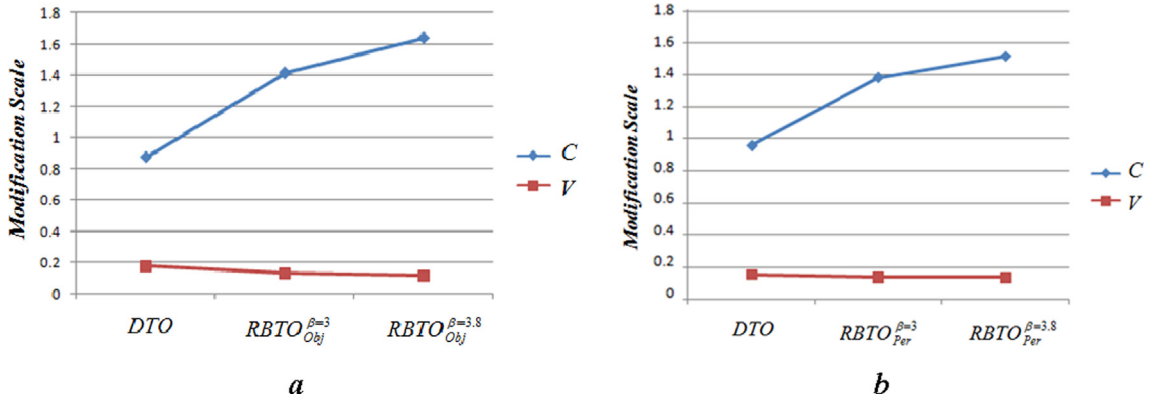

Fig. 7 Comparison between the compliance and the volume values for a) the first and b) the second categories of solutions the studied MBB beam with two holes.

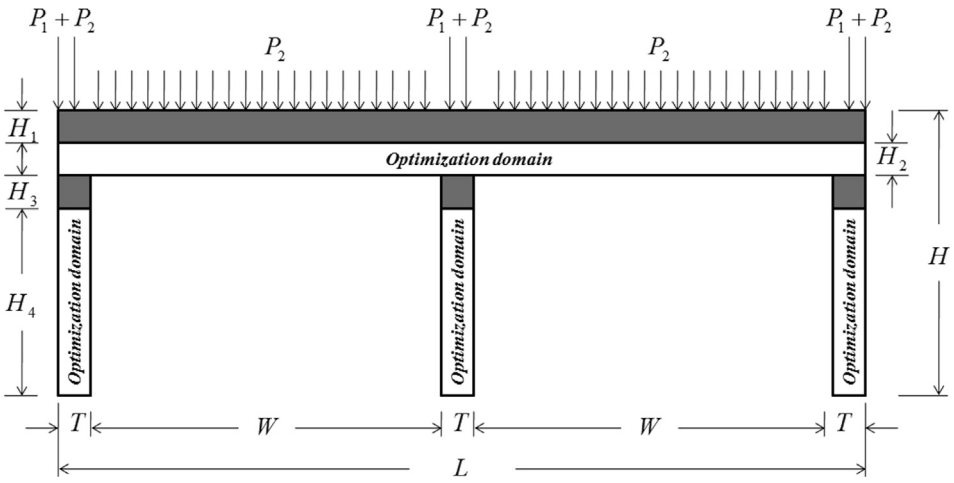

Fig. 8 Initial configuration of the studied bridge structure.

the outer geometry are: $L = 115$m and $H = 65$m. All other geometrical parameters are shown by their symbols (H_1, H_2, H_3, H_4, T and W) in Fig. 8 and the values of these symbols are presented in Table 4 in meters (see Mean Point). The third dimension (depth) equals to: $Z = 20$m. In this 3D application, there is a possibility to consider the geometry uncertainty on several number of geometrical parameters compared to the previous 2D case. The material of this bridge is steel, which has a Young's modulus $E = 200000$(MPa) and a Poisson's ratio $v = 0.3$. The material behavior is linear elastic isotropic. Two pressures are applied on the upper non-optimized domain: $P_1 = 10000$and $P_2 = 100\text{N/m}^2$. The boundary conditions are shown in Fig. 8. To perform the RBTO using Objective-Based and Performance-Based IOSF Approaches, a sensitivity evaluation is carried out on the starting point configuration and considering the central finite difference approach as an accurate tool for sensitivity analysis [34]. In this 3D model, the uncertainty is also integrated to the geometry in order to analyze its effect on the different functions (objective and performance) and to generate additional layouts.

3.2.1. First category of solutions for the studied bridge structure

The starting configuration is considered to be the failure point where the problem is to minimize the compliance subject to the volume constraint for the DTO (Eq. (1)) and also the reliability constraints for the RBTO (Eq. (5)). Optimality Criteria (OC) implemented in ANSYS Software is the used method for this kind of topology optimization problems.

Fig. 9a shows the resulting 3D bridge topologies when considering the compliance as an objective function for DTO model (failure point P_y^*). Fig. 9b and d show the resulting 3D bridge topologies when considering the compliance as an objective function for RBTO models without considering the geometry uncertainty when the target reliability indices are: $\beta_t = 3$, and $\beta_t = 3.8$, respectively. Fig. 9c and e show the resulting 3D bridge topologies when considering the compliance as an objective function for RBTO models considering the geometry uncertainty when the target reliability indices are: $\beta_t = 3$, and $\beta_t = 3.8$, respectively. The corresponding resulting compliances are shown in Table 3 for the initial configuration C^0 and the optimal one C^*. The used number of element for optimization is 132 nonlinear elements (SOLID95, 20-node).

For Fig. 9d, at $\beta_t = 3.8$ and not considering geometry uncertainty, a big difference is shown compared to the other subfigures. To consider the structural compliance as an objective function, different layout configurations can be obtained when increasing the reliability index values.

3.2.1.1. First category without considering the geometry uncertainty. The uncertainty is only considered on the material properties (E and v), the loading (P_1 and P_2) and the volume decrease ratio (V_f). The five random variables are then: E, v, P_1, P_2 and V_f. The standard deviations are assumed to be proportional to the starting values (P_y^*) presented in Table 3, i.e. $\sigma_i = \gamma_i m_i$ (Eq. (12)) where $\gamma_i = 0.1$.

When increasing the reliability index values, different topologies are obtained (Fig. 9b and d). This observation is numerically supported by the decrease of the structural volume $V(\mathbf{x})$, when increasing the reliability index values. Table 3 presents the input and output parameters of the DTO and RBTO studies for the first category of solutions for the studied 3D bridge structure without considering the geometry uncertainty. It is shown for the RBTO results that the reduction of the structural volume is almost 9.3%, while the increase of the structural compliance is almost 10%.

Fig. 10 shows the resulting sensitivity magnitude values of the compliance as an objective function with respect to the five random variables. Here, the effect of the material properties can be ignored and the volume decrease ratio V_f plays an important role in the compliance. It is found that the volume decrease ratio V_f has the biggest effect on the resulting compliance, while the Poisson's ratio has no influence on the resulting compliance as shown in Fig. 10. The effect of the volume decrease ratio is more than four times compared to the effect of pressure P_2 and more than sixteen times compared to the effect of pressure P_1.

Table 3 presents the input and output parameters when considering the compliance as an objective function. In this table, the failure point P_y^* and the optimum solution P_x^* for the two chosen target reliability indices ($\beta_t = 3$ and $\beta_t = 3.8$) are presented. The normalized vector u_i is calculated using

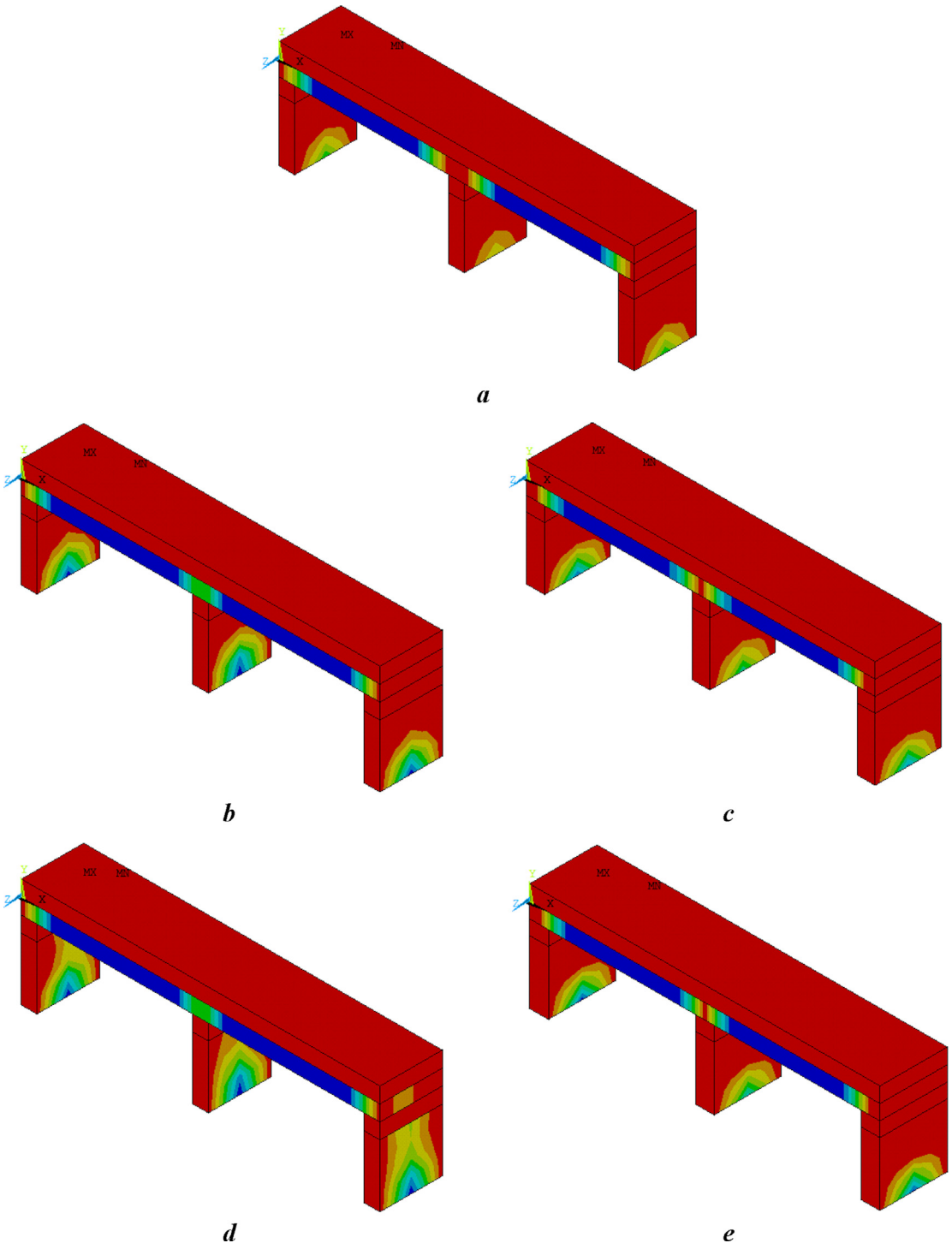

Fig. 9 Resulting 3D bridge topologies when considering the compliance as an objective function: a) DTO configuration, b) RBTO configurations for $\beta_t = 3$ without considering the geometry uncertainty, c) RBTO configurations for $\beta_t = 3$considering the geometry uncertainty, d) RBTO configuration for $\beta_t = 3.8$ without considering the geometry uncertainty, and e) RBTO configuration for $\beta_t = 3.8$ considering the geometry uncertainty.

Eq. (6) and the corresponding safety factors S_{f_i} are computed using Eq. (11).

3.2.1.2. First category when considering the geometry uncertainty. The uncertainty is considered on the geometrical dimensions (H_1, H_2, H_3, H_4, Z, T and W), the material properties (E and v), the loading (P_1 and P_2) and the compliance increase ratio (C_f). For the starting point, the used number of elements for optimization is 132 nonlinear elements (SOLID95, 20-node), while for the RBDO solutions, the used number of ele-

Table 3 Different input and output parameters for the first category of solutions for the studied 3D bridge structure without considering the geometry uncertainty.

Parameters	P_y^*	$\beta_t = 3$			$\beta_t = 3.8$		
		u_i	S_{f_i}	P_x^*	u_i	S_{f_i}	P_x^*
E(MPa)	200,000	0.10459	0.989541	197908.3	0.13248	0.986752	197350.5
ν	0.3	0	1	0.3	0	1	0.3
P_1(MPa)	10,000	0.64907	1.064907	10649.07	0.82216	1.082216	10822.16
P_2(MPa)	100	1.28326	1.128326	112.8326	1.62547	1.162547	116.2547
V_f	50	2.63078	1.263078	63.1539	3.33232	1.333232	66.66161
C^0(N.m)	19.3602×10^6	32.5209×10^6			37.9995×10^6		
C^*(N.m)	7.13953×10^6	8.80841×10^6			9.70148×10^6		
$V(\mathbf{x})$(m^3)	8750	6448.07			5847.41		

Table 4 Different input and output parameters for the first category of solutions for the studied 3D bridge structure considering the geometry uncertainty.

Parameters	P_y^*	$\beta_t = 3$			$\beta_t = 3.8$		
		u_i	S_{f_i}	P_x^*	u_i	S_{f_i}	P_x^*
H_1(m)	5	0.48862	1.048862	5.24431	0.61892	1.061892	5.309459
H_2(m)	5	0.34389	1.034389	5.171947	0.4356	1.04356	5.217799
H_3(m)	5	0.08393	1.008393	5.041964	0.10631	1.010631	5.053154
H_4(m)	20	0.76903	1.076903	21.53806	0.9741	1.09741	21.94821
Z(m)	20	1.35069	1.135069	22.70137	1.71087	1.171087	23.42174
E(MPa)	200,000	−0.0115	0.99885	199769.9	−0.01457	0.998543	199708.5
ν	0.3	0	1	0.3	0	1	0.3
P_1(MPa)	10,000	0.0714	1.00714	10071.4	0.09044	1.009044	10090.44
P_2(MPa)	100	0.14116	1.014116	101.4116	0.17881	1.017881	101.7881
T(m)	5	2.46711	1.246711	6.233554	3.125	1.3125	6.562502
W(m)	50	0.15701	1.015701	50.78507	0.19888	1.019888	50.99442
V_f	50	0.28939	1.028939	51.44696	0.36656	1.036656	51.83281
C^0(N.m)	19.3602×10^6	32.1087×10^6			36.3114×10^6		
C^*(N.m)	7.13953×10^6	11.7099×10^6			13.1751×10^6		
$V(\mathbf{x})$(m^3)	8750	11295.7			12037.3		

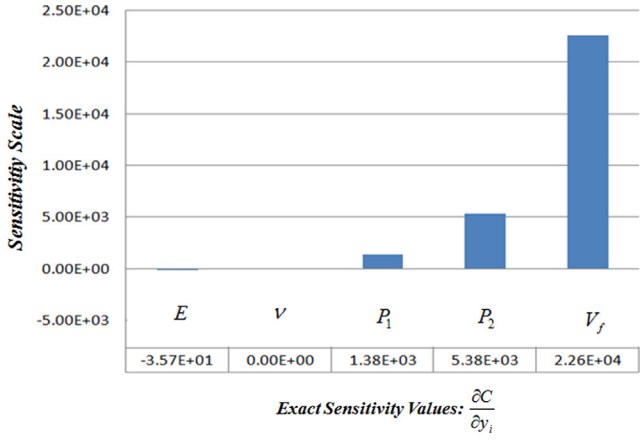

Fig. 10 Sensitivity magnitude values of the compliance as an objective function without considering the geometry uncertainty.

ments for optimization is 192 nonlinear elements (SOLID95, 20-node). The 12 random variables are then: H_1, H_2, H_3, H_4, Z, E, ν, P_1, P_2, T, $W$and V_f. The standard deviations are assumed to be proportional to the starting values (P_y^*) presented in Table 4, i.e. $\sigma_i = \gamma_i m_i$ (Eq. (12)) where $\gamma_i = 0.1$.

Table 4 presents the input and output parameters of the DTO and RBTO studies for the first category of solutions for the studied 3D bridge structure considering the geometry uncertainty. The numerical results in Table 4 show that the structural volume $V(\mathbf{x})$ increases when increasing the reliability index values. It is shown that the increase of the structural volume is almost 6.6%, while the increase of the structural compliance is almost 13%.

Fig. 11 shows the sensitivity values of the compliance as an objective function with respect to the 12 random variables. Here, the effect of the material properties can be ignored and the geometrical parameters play the most important role with different degrees. It is also found that the thickness T has the biggest effect on the resulting compliance, while the Poisson's ratio has no influence on the resulting compliance

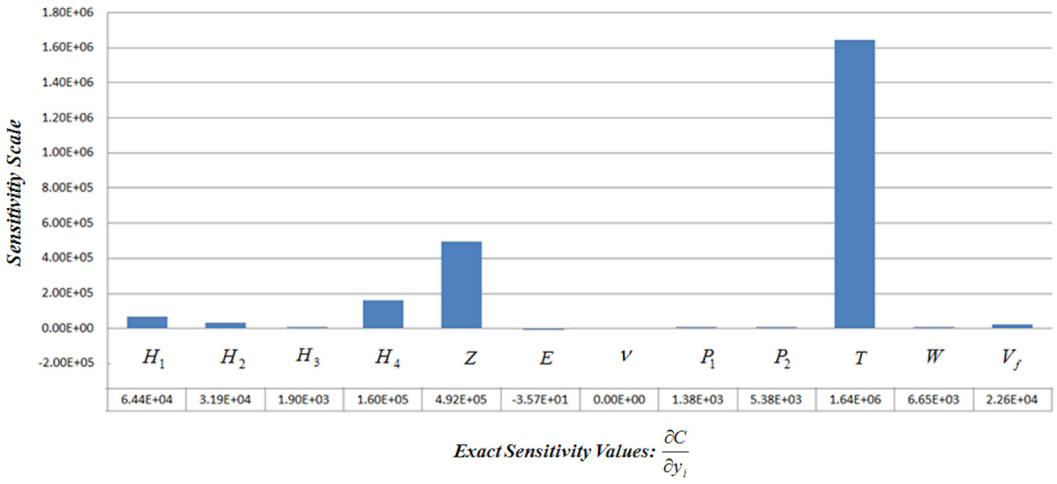

Fig. 11 Sensitivity magnitude values of the compliance as an objective function considering the geometry uncertainty.

as shown in Fig. 11. The effect of the thickness T is more than three times of the third dimension Z. The compliance sensitivity with respect to the height of support part H_3 is the lowest value between the geometrical parameters. This value is even lower than the compliance sensitivity with respect to the pressure P_2. This way it is difficult to say that all geometrical parameters play the most important role in the structural compliance.

3.2.2. Second category of solutions for the studied bridge structure

The starting configuration is considered to be the failure point where the problem is to minimize the structural volume subject to the compliance constraint for the DTO (Eq. (2)) and also the reliability constraints for the RBTO (Eq. (8)). Sequential Convex Programming (SCP) implemented in ANSYS Software is the used method for this kind of topology optimization problems.

Fig. 12a shows the resulting 3D bridge topologies when considering the compliance as a performance function for DTO model (failure point P_y^*). Fig. 12b and d show the resulting 3D bridge topologies when considering the compliance as a performance function for RBTO models without considering the geometry uncertainty when the target reliability indices are: $\beta_t = 3$, and $\beta_t = 3.8$, respectively. Fig. 12c and e show the resulting 3D bridge topologies when considering the compliance as a performance function for RBTO models considering the geometry uncertainty when the target reliability indices are: $\beta_t = 3$, and $\beta_t = 3.8$, respectively. The corresponding resulting volumes are shown in Table 4 for the initial configuration V^0 and the optimal one V^*. When starting from Fig. 12a, the change of the material distribution layouts in all other figures due to the change of reliability index values is related with the application of geometry uncertainty. Fig. 12d possesses a small change in the material distribution compared to Fig. 12b. The same observation can be noted when comparing Fig. 12e and c. In the literature, to consider the structural volume as an objective function, the introduction of reliability concept may not affect the geometrical description of the layouts [25]. However, Fig. 12c and e show that both IOSF approaches provide different layouts that can be helpful to designers.

3.2.2.1. Second category without considering the geometry uncertainty. The uncertainty is only considered on the material properties (E and ν), the loading (P_1 and P_2) and the compliance increase ratio (C_f). The used number of elements for optimization is 132 nonlinear elements (SOLID95, 20-node). The five random variables are then: E, ν, P_1, P_2 and C_f. The standard deviations are assumed to be proportional to the starting values (P_y^*) presented in Table 5, i.e. $\sigma_i = \gamma_i m_i$ (Eq. (12)) where $\gamma_i = 0.1$

Table 5 presents the input and output parameters of the DTO and RBTO studies for the second category of solutions, for the studied 3D bridge structure without considering the geometry uncertainty. It is shown for the RBTO results that the reduction of the structural volume is almost 1.6%, while the increase of the structural compliance is almost 5.1%. In this table, the failure point P_y^* and the design point P_x^* for the two chosen target reliability indices ($\beta_t = 3$ and $\beta_t = 3.8$) are presented. The normalized vector u_i is calculated using Eq. (9) and the corresponding safety factors S_{f_i} are computed using Eq. (11). The numerical results in Table 5 show that the optimal values of the structural volume V^* decrease when increasing the reliability index values.

Fig. 13 shows the sensitivity values of the compliance as a performance function with respect to the five random variables. Here, the effect of the material properties can be ignored and the compliance increase ratio C_f plays an important role in the compliance. It is found that the compliance increase ratio C_f has the biggest effect on the resulting compliance, while the Poisson's ratio has no influence on the resulting compliance as shown in Fig. 13. The effect of the compliance increase ratio is more than five times compared to the effect of pressure P_2.

3.2.2.2. Second category when considering the geometry uncertainty. The uncertainty is considered on the geometrical dimensions (H_1, H_2, H_3, H_4, Z, T and W), the material properties (E and ν), the loading (P_1 and P_2) and the compliance increase ratio (C_f). For the starting point, the used number of elements for optimization is 132 nonlinear elements (SOLID95, 20-node), while for the RBDO solutions, the used number of elements for optimization is 192 nonlinear elements (SOLID95, 20-node). The 12 random variables are then: H_1, H_2, H_3, H_4,

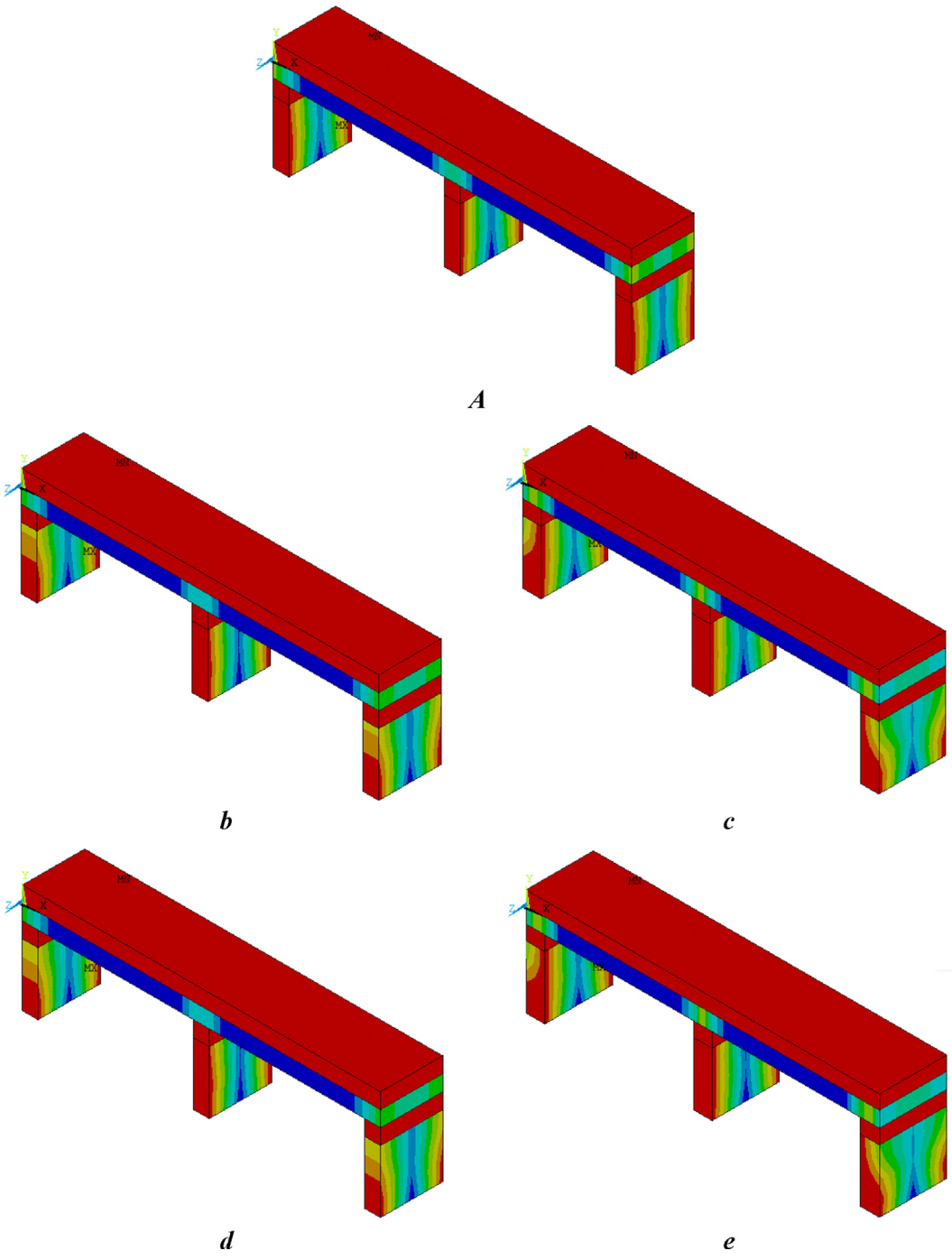

Fig. 12 Resulting 3D bridge topologies when considering the compliance as a performance function: a) DTO configuration, b) RBTO configurations for $\beta_t = 3$ without considering the geometry uncertainty, c) RBTO configurations for $\beta_t = 3$considering the geometry uncertainty, d) RBTO configuration for $\beta_t = 3.8$ without considering the geometry uncertainty, and e) RBTO configuration for $\beta_t = 3.8$ considering the geometry uncertainty.

Z, E, v, P_1, P_2, T, $W$and C_f. The standard deviations are assumed to be proportional to the starting values (P_y^*) presented in Table 6, i.e. $\sigma_i = \gamma_i m_i$ (Eq. (12)) where $\gamma_i = 0.1$

Table 6 presents the input and output parameters of the DTO and RBTO studies for the second category of solutions, for the studied 3D bridge structure considering the geometry uncertainty. The numerical results in Table 6 show that the optimal values of the structural volume V^* increases when increasing the reliability index values. It is shown that the increase of the structural volume is almost 9.2%, while the increase of the structural compliance is almost 12%.

Fig. 14 shows the sensitivity values of the compliance as a performance function with respect to the 12 random variables. Here, the effect of the material properties can be ignored and the geometrical parameters play the most important role with different degrees. It is also found that the thickness T has the

Table 5 Different input and output parameters for the second category of solutions for the studied 3D bridge structure without considering the geometry uncertainty.

Parameters	P_y^*	$\beta_t = 3$			$\beta_t = 3.8$		
		u_i	S_{f_i}	P_x^*	u_i	S_{f_i}	P_x^*
E(MPa)	200,000	0.07416	0.992584	198516.8	0.09394	0.990606	198121.2
v	0.3	0	1	0.3	0	1	0.3
P_1(MPa)	10,000	0.45392	1.045392	10453.92	0.57497	1.057497	10574.97
P_2(MPa)	100	1.18127	1.118127	111.8127	1.49628	1.149628	114.9628
C_f	50	2.71902	1.271902	63.59508	3.44409	1.344409	67.22043
V^0(m^3)	17,500	17,500			17,500		
V^*(m^3)	4052.43	3785.73			3725.33		
C(**x**)(N.m)	10.4453×10^6	12.6581×10^6			13.2987×10^6		

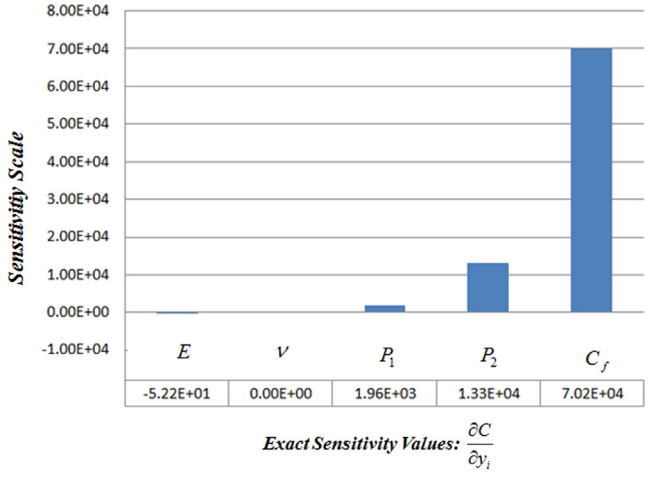

Fig. 13 Sensitivity values of the compliance as a performance function without considering the geometry uncertainty.

biggest effect on the resulting compliance, while the Poisson's ratio has no influence on the resulting compliance as shown in Fig. 14. The effect of the thickness T is more than three times of the third dimension Z. The compliance sensitivity with respect to the height of the upper beam H_1 is negative. The compliance sensitivity with respect to the height of support part H_3 is the lowest magnitude value between the geometrical parameters. This last value is lower than the compliance sensitivity with respect to the pressure P_2. So, the sensitivities with respect to the geometrical parameters can be negative or positive depending on the used approach.

Fig. 15a and b show a comparison between the compliance and the volume values for the first categories of solutions without considering and when considering the geometry uncertainty, respectively. Fig. 15c and d show a comparison between the compliance and the volume values for the second categories of solutions without considering and when considering the geometry uncertainty, respectively. In Fig. 15a, b, c and d, the volume values are divided by 10^3 m^3, while the compliance values are divided by 10^6N.m. It is shown in Fig. 15a and

Table 6 Different input and output parameters for the second category of solutions for the studied 3D bridge structure considering the geometry uncertainty.

Parameters	P_y^*	$\beta_t = 3$			$\beta_t = 3.8$		
		u_i	S_{f_i}	P_x^*	u_i	S_{f_i}	P_x^*
H_1(m)	5	−0.15357	0.984643	4.923215	−0.19452	0.980548	4.902739
H_2(m)	5	0.61428	1.061428	5.30714	0.77809	1.077809	5.389045
H_3(m)	5	0.08866	1.008866	5.044332	0.11231	1.011231	5.056154
H_4(m)	20	0.69767	1.069767	21.39534	0.88372	1.088372	21.76743
Z(m)	20	1.37238	1.137238	22.74476	1.73835	1.173835	23.4767
E(MPa)	200,000	−0.0117	0.99883	199,766	−0.01482	0.998518	199703.6
v	0.3	0	1	0.3	0	1	0.3
P_1(MPa)	10,000	0.0716	1.00716	10071.6	0.0907	1.00907	10090.7
P_2(MPa)	100	0.18633	1.018633	101.8633	0.23602	1.023602	102.3602
T(m)	5	2.4357	1.24357	6.217851	3.08522	1.308522	6.542611
W(m)	50	0.25389	1.025389	51.26947	0.3216	1.03216	51.608
C_f	50	0.4289	1.04289	52.14449	0.54327	1.054327	52.71636
V^0(m^3)	17,500	23706.5			25572.2		
V^*(m^3)	4052.43	6011.56			6568.38		
C(**x**)(N.m)	10.4453×10^6	16.87743×10^6			18.9504×10^6		

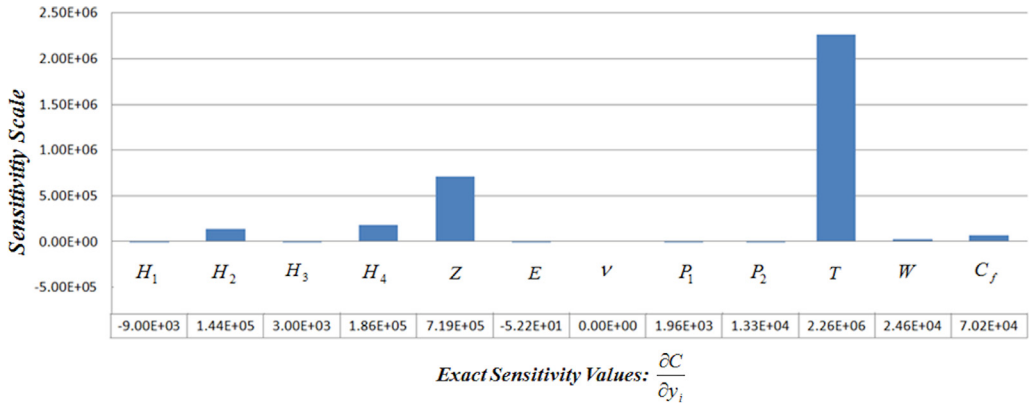

Fig. 14 Sensitivity values of the compliance as a performance function considering the geometry uncertainty.

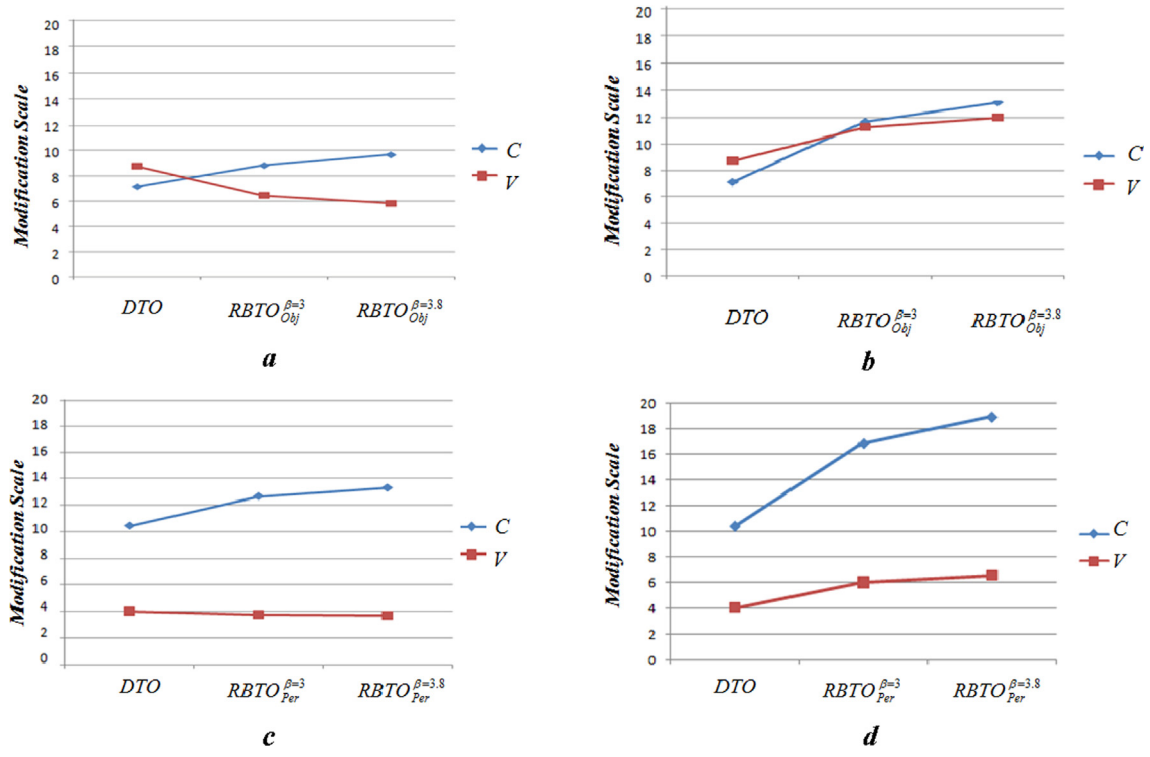

Fig. 15 Comparison between the compliance and the volume values for the first categories of solutions a) without considering and b) when considering the geometry uncertainty and for the second categories of solutions c) without considering and d) when considering the geometry uncertainty.

c that when increasing the reliability index values, the structural compliance values increases, while the structural volume decreases. However, it is not the same findings in Fig. 15b and d. The geometry uncertainty affects the behavior of the objective and performance functions where the increase of the reliability index values leads to an increase of both functions (objective and performance).

As result, when using the Objective-Based IOSF Approach, the compliance is treated as an objective function. In this case, two studied are carried out. The first study does not consider the uncertainty on the geometry. So, the sensitivity is evaluated with respect to five parameters (Fig. 10). The resulting RBTO configurations can be modeled with different layouts for the next stage (detailed design). However, the second study is to consider the uncertainty on the geometry. So, the sensitivity is evaluated with respect to 12 parameters (Fig. 11). The resulting RBTO configurations can be modeled with similar layouts for the next stage (detailed design). Here, there is no significant effect of the geometry uncertainty for this example. For the Performance-Based IOSF Approach, the compliance is treated as a performance function. In this case, two studies are carried out. The first study is to not consider the uncertainty on the geometry. So, the sensitivity is evaluated with respect to five parameters (Fig. 13). However, the second study is to consider

the uncertainty on the geometry. So, the sensitivity is evaluated with respect to 12 parameters (Fig. 14). The geometry uncertainty can affect the layouts for both approaches.

In the case of the ignorance of the geometry uncertainty, the structural compliance increases while the structural volume decreases when increasing the reliability index values. This result is similar to the first RBTO findings [4-7]. In contrast, when considering the geometry uncertainty, both of structural compliance and volume values increase when the reliability index values increase. This result can be considered as a main observation of this work. It can be as a basic idea to develop a new strategy combining the different findings of the developments from both points of view 'reliability and topology'.

4. Conclusion

In this work, two alternative approaches based on the Inverse Optimum Safety Factor (IOSF) are developed; Objective-Based IOSF Approach and Performance-Based IOSF Approach. Moreover, a comparison between the two approaches was conducted considering the effect of different parameters such as geometry, material properties, and loadings. A 2D finite element model of a simple MBB beam with two holes, and a 3D finite element model are presented. In the 2D model, the uncertainty of the input parameters (loading and material properties) and the output parameters (volume decrease ratio or compliance increase ratio) are considered. Moreover, the geometry uncertainty of the 3D model is added to show its effect on the different functions (compliance and volume).

The studied 3D case gives the opportunity to apply the uncertainty on several geometrical parameters without affecting the structure performance, while to apply the uncertainty of the dimensions of the MBB beam or its two holes can affect the boundary conditions and then the structure performance. The resulting layouts from both IOSF approaches can cover the different developments in the literature where two alternative options can be found: The first choice is to consider the structural compliance as an objective function that can lead to different geometrical descriptions. The second choice is to consider the structural volume as an objective function that leads to the same geometrical descriptions as mentioned in the literature, but when considering the geometry uncertainty, it can provide different layouts.

As a result, it is very important to use both alternative approaches when dealing with this kind of problems during the conceptual design stage in order to open more categories of solutions as layouts for the detailed design stage. When increasing the reliability index values, the Objective-Based IOSF Approach leads to different RBDO layouts for the studied MBB beam with two holes compared to the DTO layout, while the Performance-Based IOSF Approach leads to different RBDO layouts for the studied 3D bridge structure compared to the DTO layout. Thus, reliability-based topology optimization using both developed approaches is able to generate two groups of solutions, giving the designer a range of topologies. Taking the geometry uncertainty into account, it is possible to produce different RBTO layouts. In which this can also change the relationship between the output parameters. This work can be extended to nonlinear distribution laws (lognormal, uniform, Weibull, Gumbel ...). This work provides a detailed RBTO model that considers the uncertainty of inputs and generates several design alternatives in the conceptual design phase. The uncertainty on the geometrical parameters plays an important role on the behavior of the objective and performance functions when increasing the reliability index values.

Declaration of Competing Interest

The authors declare that they have no known competing financial interests or personal relationships that could have appeared to influence the work reported in this paper.

References

[1] M.P. Bendsøe, N. Kikuchi, Generating optimal topologies in optimal design using a homogenization method, Comp. Meth. Appl. Mech. Engrg. 71 (1988) 197–224.

[2] L. Xia, (2016): Multiscale Structural Topology Optimization, ISTE & Elsevier, ISBN: 9781785481000, pp 184, April 2016.

[3] W. Zhang, J. Zhu, T. Gao (2016): Topology Optimization in Engineering Structure Design, ISTE & Elsevier, ISBN: 9781785482243, pp 294, October 2016.

[4] G. Kharmanda, N. Olhoff, (2001): Reliability-Based Topology Optimization, Report N°: 110, Institute of Mechanical Engineering, Aalborg University, Denmark, December (2001).

[5] G. Kharmanda, N. Olhoff, Reliability-Based Topology Optimization as a New Strategy to Generate Different Topologies, in: E. Lund, N. Olhoff, J. Stegmsen (Eds.), the Nordic Seminar in Computational Methods, Aalborg University, Denmark, 2002.

[6] G. Kharmanda, N. Olhoff, A. Mohamed, M. Lemaire, (2004): Reliability-Based Topology Optimization, Journal of Structural and Multidisciplinary Optimization 26 (2004) 295–307.

[7] G. Kharmanda, S. Lambert, N. Kourdi, A. Daboul, A. Elhami, Reliability-based topology optimization for different engineering applications, International Journal of CAD/CAM 7 (2007) 61–69.

[8] G. Kharmanda, A. El-Hami, I. Antypas (2019): Inverse optimum safety factor method as an effective tool for reliability-based topology optimization: Application on static and dynamic cases, in: Fifth International Conference on Soft Computing & Optimisation in Civil, Structural and Environmental Engineering, Riva del Garda, near Lake Garda, Italy, 16-19 September 2019.

[9] G. Kharmanda, A. El-Hami (2017): Biomechanics: Optimization, Uncertainties and Reliability, ISTE & Wiley, ISBN: 9781786300256, January 2017.

[10] G. Kharmanda, I. Antypas, A. Dyachenko, Inverse Optimum Safety Factor Method for Reliability-Based Topology Optimization Applied to Free Vibrated Structures, Journal of Engineering Technologies and Systems 29 (1) (March 2019) 8–19.

[11] K. Bae, S. Wang (2002), Reliability-based topology optimization, in: Proceedings of 9th AIAA/ISSMO Symposium on Multidisciplinary Analysis and Optimization 2002, AIAA 2002-5542.

[12] H.S. Jung, S. Cho, Y.S. Yang (2003): Reliability-based Robust Topology Design Optimization of Nonlinear Structures, WCSMO5, Italy, 2003.

[13] A. Tovar, G.L. Niebur, M. Sen, J.E. Renaud (2004): Bone Structure Adaptation as a Cellular Automaton Optimization Process, In: 45th AIAA/ASME/ASCE/AHS/ASC Structures, Structural Dynamics and Materials Con-ference, Palm Springs, CA.

[14] S. Gowid, R. Dixon, S. Ghani, Profitability, reliability and condition based monitoring of LNG floating platforms: A review, J. Nat. Gas Sci. Eng. 7 (2015) 1495–1511.
[15] N.M. Patel, H. Agarwal, A. Tovar, J. Renaud, Reliability based topology optimization using the hybrid cellular automaton method, 1st AIAA Multidisciplinary Design Optimization Specialist Conference, 2005.
[16] Y.S. Eom, K.S. Yoo, J.Y. Park, S.Y. Han, Reliability-based topology optimization using a standard response surface method for three-dimensional structures, Journal of Structural and Multidisciplinary Optimization 43 (2) (2011) 287–295.
[17] M. Jalalpour, M. Tootkaboni, An efficient approach to reliability-based topology optimization for continua under material uncertainty, Journal of Structural and Multidisciplinary Optimization 53 (4) (2016) 759–772.
[18] J. Patel, S.K. Choi, Classification approach for reliability-based topology optimization using probabilistic neural networks, Journal of Structural and Multidisciplinary Optimization 45 (4) (2012) 529–543.
[19] L. Wang, D. Liu, Y. Yang, X. Wang, Z. Qiu (2017): A novel method of non-probabilistic reliability-based topology optimization corresponding to continuum structures with unknown but bounded uncertaintie Computer Methods in Applied Mechanics and Engineering, 326, pp 573-595, 2017.
[20] Y. Aoues, A. Chateauneuf, Benchmark study of numerical methods for reliability-based design optimization, Struct Multidisc Optim 41 (2010) 277–294.
[21] G. Kharmanda, N. Olhoff, A. El-Hami, Optimum values of structural safety factors for a predefined reliability level with extension to multiple limit states, Struct. Multidiscip. Optim. 27 (2004) 421–434.
[22] G. Kharmanda, M.-H. Ibrahim, A. Abo Al-kheer, F. Guerin, A. El Hami, Reliability-Based Design Optimization of Shank Chisel Plough Using Optimum Safety Factor Strategy, Journal of Computers and Electronics Agriculture 109 (2014) 162–171.
[23] R.J. Yang, C. Chuang, L. Gu, G. Li, Experience with approximate reliability-based optimization methods II: an exhaust system problem, Struct Multidisc Optim 29 (2005) 488–497.
[24] B. Radi, A. Makhloufi, E. El-Hami, M. Sbaa, Optimization Safety Factors to Study an Ultrasonic Motor, Int. J. Simul. Multidisci. Des. Optim. 4 (2010) 71–76.
[25] C.K. Mozumder, N.M. Patel, D. Tillotson, J.E. Renaud, An Investigation of Reliability-based Topology Optimization, in: 11th AIAA/ISSMO Multidisciplinary Analysis and Optimization Conference 6-8 September 2006, Portsmouth, Virginia.
[26] M.P. Bendsøe, Optimal shape design as a material distribution problem, Struct. Optim. 1 (1989) 193–202.
[27] N. Ahmad, Q. Ali, H. Crowley, R. Pinho, Earthquake loss estimation of residential buildings in Pakistan, Nat. Hazards 73 (3) (2014) 1889–1955.
[28] N. Ahmad, A. Shahzad, Q. Ali, M. Rizwan, A.N. Khan, Seismic fragility functions for code compliant and non-compliant RC SMRF structures in Pakistan, Bull. Earthq. Eng. 16 (10) (2018) 4675–4703.
[29] J. Jeppsson, Reliability-based assessment procedures for existing concrete structures PhD dissertation, Division of Structural Engineering, Lund University, 2003.
[30] M. Lemaire, Structural Reliability, ISTE, London and John Wiley & Sons, New York, 2009.
[31] G. Kharmanda, A. Shokry, S. Gowid, A. El-Hami, Comparison of two points of view when developing reliability-based topology optimization model: Validation on fatigue damage analysis, Journal of Uncertainties and Reliability of Multiphysical Systems 19–3 (1) (December 2019).
[32] O. Sigmund, A 99 line topology optimization code written in MATLAB, Struct Multidiscipl Optim 21 (2) (2001) 120–127.
[33] M.H. Ibrahim, G. Kharmanda, A. Charki, Reliability-based design optimization for fatigue damage analysis, The International Journal of Advanced Manufacturing Technology 76 (2015) 1021–1030.
[34] G. Kharmanda, S. Gowid, E. Mahdi, A. Shokry, Efficient System Reliability-Based Design Optimization Study for Replaced Hip Prosthesis Using New Optimized Anisotropic Bone Formulations, Materials 13 (2) (January 2020) 1–17.
[35] G. Kharmanda, A. El-Hami (2016): Reliability in Biomechanics, ISTE & Wiley, ISBN: 9781786300249, pp 266, November 2016.